OCVD carrier lifetime in P^+NN^+ diode structures with axial carrier lifetime gradient

V. Benda [a,*], M. Cernik [b], V. Papez [a]

[a] *Department of Electrotechnology, Czech Technical University in Prague, Technicka 2, 166 27 Praha 6, Czech Republic*
[b] *Department of Mechatronics, Technical University Liberec, Liberec, Czech Republic*

Abstract

The OCVD (open circuit voltage decay) method is the generally used method for the determining of carrier lifetime in the structures of semiconductor devices. This paper is focused on power diode (P^+NN^+) structures, in which is realised a carrier lifetime gradient to influence the current and voltage waveforms during the reverse recovery process. A theoretical analysis of the general features of voltage decay courses in OCVD measurements on diode structures with an axial carrier lifetime gradient in the diode base is presented. Some results obtained from both simulations and experimental measurements are discussed in the paper.
© 2005 Elsevier Ltd. All rights reserved.

Keywords: OCVD method; Carrier lifetime gradient; Power diode structures

1. Introduction

The OCVD (open circuit voltage decay) method is a commonly used technique for carrier lifetime measurements in the structures of semiconductor devices. The measurement is relatively very simple: a diode part of a device is forward biased and then the circuit is opened. OCVD carrier lifetime τ_{eff} is determined from the slope of the voltage decay [1]

$$\tau_{\text{eff}} = -\frac{kT}{e}\left(\frac{\mathrm{d}V}{\mathrm{d}t}\right)^{-1}. \tag{1}$$

It depends on carrier lifetime τ in the base of the diode structure, injection level, and on several more parameters.

The simple formula (1) assumes a low injection level, uniform carrier lifetime distribution across the diode base region and disregards space charge effects. Nevertheless, the method is used generally. This paper focuses on interpretation results of OCVD measurements for diode structures with an axial carrier lifetime gradient in the diode base.

* Corresponding author. Tel.: +420 224352163; fax: +420 224353949.
E-mail address: benda@fel.cvut.cz (V. Benda).

2. The OCVD method

In a simple approximation, the voltage drop across a P^+NN^+ diode structure $V(t)$ is given by

$$V(t) = V_P(t) + V_N(t) - \int_0^w E(x;t)\mathrm{d}x, \tag{2}$$

where V_P is the voltage drop at the P^+N junction, V_N is the voltage drop at the NN^+ junction and E is a local electric field in the base of diode structure

$$E(x;t) = \frac{J(x;t)}{e(\mu_n + \mu_p)\Delta n(x;t)} - \frac{kT(\mu_n - \mu_p)}{e(\mu_n + \mu_p)\Delta n(x;t)}$$
$$\times \frac{\mathrm{d}\Delta n(x;t)}{\mathrm{d}x}. \tag{3}$$

The junction voltages can be derived using the Boltzmann relations

$$\frac{p_N(0;t)}{N_A^+} = \exp\left\{\frac{-e[\varphi_P - V_P(t)]}{kT}\right\}, \tag{4a}$$

$$\frac{n_N(w;t)}{N_D^+} = \exp\left\{\frac{-e[\varphi_N - V_N(t)]}{kT}\right\}, \tag{4b}$$

$\varphi_P = (kT/e)\ln(N_A^+ N_D/n_i^2)$, $\varphi_N = (kT/e)\ln(N_D N_N^+/n_i^2)$ are the built-in voltages at P^+N and NN^+ junctions.

Assuming a homogeneous carrier lifetime τ distribution (i.e. a constant carrier lifetime), carrier concentration at the junctions decreases due to recombination as

$$p_N(0;t) = p_N(0;0)\exp\left(-\frac{t}{\tau}\right), \qquad (5a)$$

$$n_N(w;t) = n_N(w;0)\exp\left(-\frac{t}{\tau}\right). \qquad (5b)$$

If internal electric field in the base of the diode can be neglected, from (2) and (4) it follows that the carrier lifetime under high injection conditions may be expressed by the well-known formula

$$\tau = -2\frac{kT}{e}\left(\frac{dV}{dt}\right)^{-1}. \qquad (6)$$

Comparing (6) and (1), for the high injection carrier lifetime follows $\tau = 2\tau_{eff}$.

Under low injection conditions ($V_N \approx 0$) it can be found for carrier lifetime $\tau_{eff} = \tau$, because in this case

$$\tau = -\frac{kT}{e}\left(\frac{dV}{dt}\right)^{-1}. \qquad (7)$$

Eqs. (6) and (7) are often used for determining both high-injection and low-injection carrier lifetime by the OCVD method and evaluation of the carrier lifetime dependence on injection level.

3. Influence of axial carrier lifetime gradient

In real cases, recombination in the highly doped region should be considered [2]. Formulae (6) and (7) were derived under the assumption that the contribution of the internal electric field given by (3) can be neglected. This is a good approximation in the case of a homogenous diode structure, but in the case of existence of an axial carrier lifetime gradient in the base of the diode structure, the use of (6) and (7) for determining carrier lifetime from the voltage decay is rather problematic.

If carrier lifetime is not a constant, the recombination rate of excess carrier concentration at P^+N and NN^+ junction differs.

Assuming $p_N(0;t) = p_N(0;0)\exp(-(t/\tau_P))$ and $n_N(w;t) = n_N(w;0)\exp(-(t/\tau_N))$, and neglecting the voltage drop due to the internal electric field, the post-injection voltage decay under high injection conditions can be approximated by

$$\frac{dV}{dt} = -\frac{kT}{e}\left(\frac{1}{\tau_P} + \frac{1}{\tau_N}\right). \qquad (8)$$

Using $(1/\tau_{eff}) = (1/\tau_P) + (1/\tau_N)$ for an effective carrier lifetime, it can be found that for $\tau_P \ll \tau_N$ the effective high injection carrier lifetime is $\tau_{eff} \approx \tau_P$, and for $\tau_N \ll \tau_P$ the effective carrier lifetime is $\tau_{eff} \approx \tau_N$. This strongly differs from the case of uniform carrier lifetime distribution, where $\tau_{eff} = 0.5\tau$, as follows from (6). From (8) it also follows that the application Eqs. (6) and (7) for evaluation the carrier lifetime dependence on injection level from OCVD measurements in

the case of structures with an axial carrier lifetime gradient (used e.g. in [4]) may not be correct.

Another important factor that can influence the voltage decay after opening the circuit is an internal electric field connected with the excess carrier concentration gradient that originates due to differences in the recombination rate along the device structure. From (3) it follows that during OCVD measurements this electric field can be approximated as

$$E(x;t) = -\frac{kT(\mu_n - \mu_p)}{e(\mu_n + \mu_p)\Delta n(x;t)}\frac{d\Delta n(x;t)}{dx}. \qquad (9)$$

An analytical solution of the transient process is relatively very complicated. To evaluate the influence of the internal electric field on the open circuit voltage decay, numerical simulations of the transient process were performed.

4. Simulation results and discussion

The DIMOWIN programme [5] was used for the numerical simulation of the transient process. This programme allows one-dimensional simulations of both reverse recovery process and OCVD measurements under both homogeneous and inhomogeneous carrier lifetime distributions in the base of P^+NN^+ diode structures (abrupt $P+N$ and $N+N$ junctions are supposed). In the case of the inhomogeneous carrier lifetime distribution, the carrier lifetime distribution is supposed in the form

$$\tau(x) = \tau(0)\exp(-\alpha x). \qquad (10)$$

(τ is the high injection carrier lifetime in the Shockley–Read–Hall approximation). The programme can be used for an extensive range of physical diode parameters and operating conditions.

In our simulations, we looked for the influence of the carrier lifetime gradient in the diode base on the course of voltage decay under conditions of OCVD measurements. To obtain comparisons of parameters, the mean value of the carrier lifetime $\bar{\tau}$ was kept constant

$$\bar{\tau} = \frac{\tau(0)}{w}\int_0^w \exp(-\alpha x)dx = \frac{\tau(0)}{\alpha w}[1 - \exp(-\alpha w)]. \qquad (11)$$

To demonstrate the influence of the axial carrier lifetime gradient on the OCVD process, a P^+NN^+ diode structure of the N type base thickness of 300 μm was used. An example of carrier lifetime distribution in the diode base used for simulations is shown in Fig. 1. For individual cases, the distribution of excess carriers in the steady-state forward biased conditions is calculated. The excess carrier distributions at the current density 10 A/cm^2 for different carrier lifetime distributions (shown in Fig. 1) are shown in Fig. 2.

The numerical simulation of the change of carrier distribution in the diode base after opening the circuit shows that under conditions of an axial carrier lifetime gradient there is also a relatively high concentration gradient of excess carriers in the diode base during the transient process.
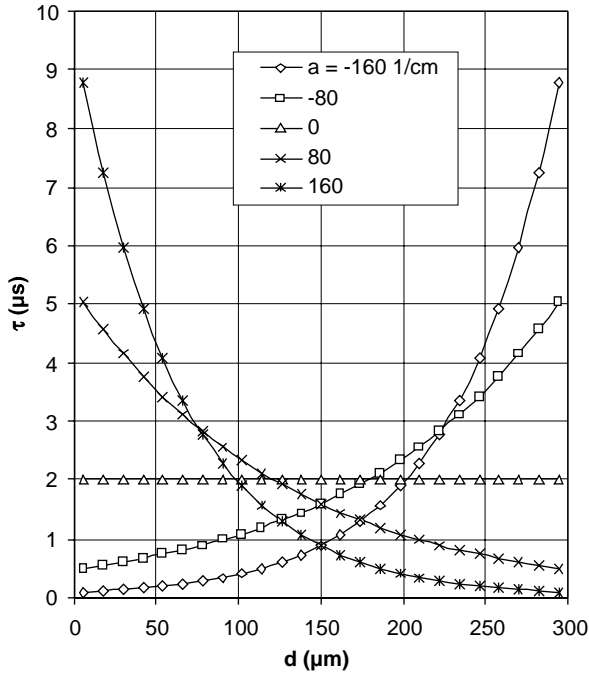
Fig. 1. Examples of carrier lifetime distribution used for simulation using programme DIMOVIN. The mean value of carrier lifetime $\bar{\tau} = 2$ μs is assumed.

Examples of changes of excess carrier concentration distribution are shown in Fig. 3. An internal electric field is connected with the excess carrier concentration gradient and it also has a considerable influence on the effective carrier lifetime τ_{eff} measured by the OCVD method and calculated from (1).
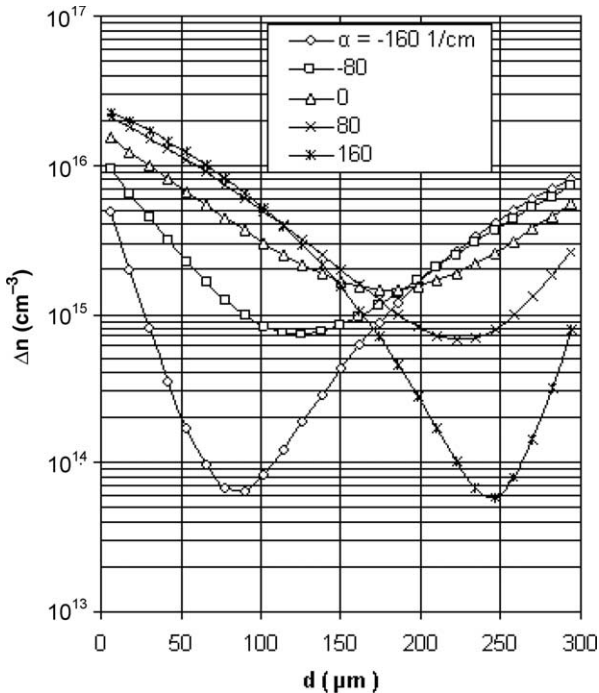

Fig. 2. Examples of excess carrier distribution at the on-state carrier density $J_F = 10$ A/μs for carrier lifetime profiles shown in Fig. 1 ($\bar{\tau} = 2$ μs).
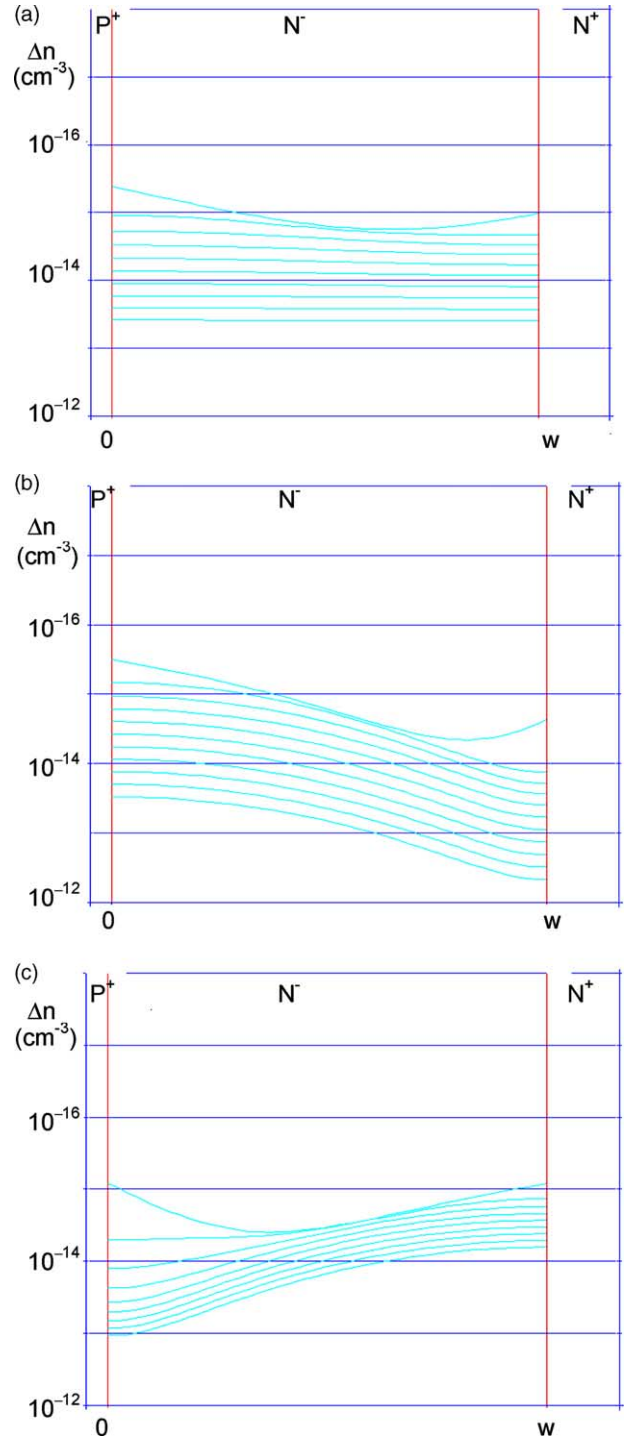

Fig. 3. Examples of excess carrier distribution during OCVD carrier lifetime measurement. (a) $\tau = $ constant; (b) $\tau_P > \tau_N$; (c) $\tau_P < \tau_N$.

From the excess carrier distribution after opening circuit V_P and V_N were calculated using (4a) and (4b) and the voltage δV originating due to the excess carrier gradient

$$\delta V(t) = \int_0^w -E(x;t)\mathrm{d}x, \tag{12}$$

where $E(x;t)$ is given by (9). The voltage drop $V(t)$ across the diode is given by

$$V(t) = V_P(t) + V_N(t) + \delta V(t). \tag{13}$$

Examples of waveforms $V_P(t)$, $V_N(t)$, $\delta V(t)$ and $V(t)$ for the same mean carrier lifetime $\bar{\tau} = 2\ \mu m$ and different α (determining the carrier lifetime gradient) are shown in Fig. 4. On-state current density 10 A/cm^2 was used for the simulations.

From the simulations it follows, that in homogeneous structures with a constant carrier lifetime the internal electric field is very low and does not influence the voltage decay. At the beginning of the process, carriers diffuse into the central part of the diode structure. This results in a higher decrease of excess carriers at junctions than only due to recombination. Within a short time, the carrier distribution becomes nearly constant and the voltage decay can be well described by (6), for the end of the process by (7), in a very good agreement with [2] and [3].
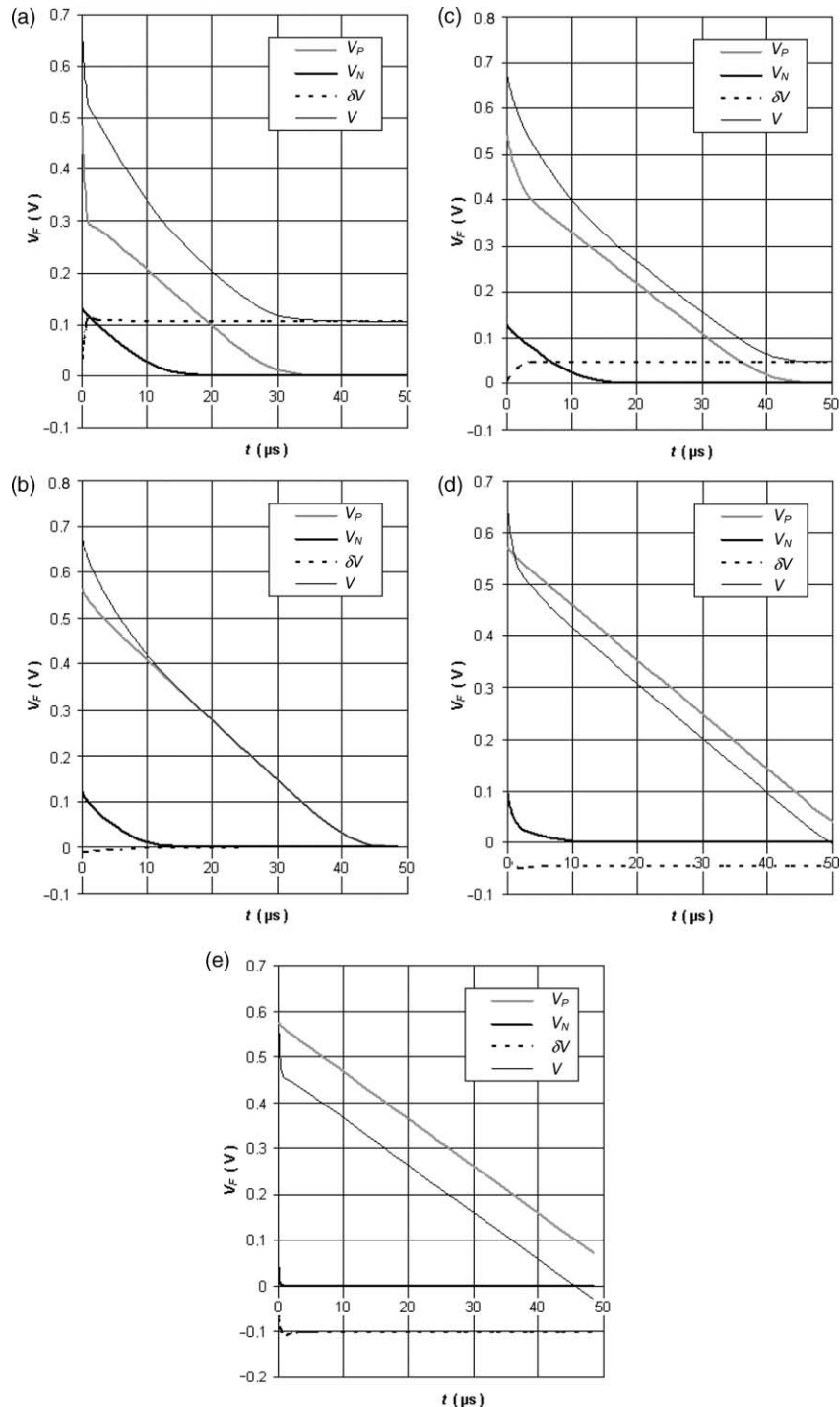

Fig. 4. Examples of voltage V, V_P, V_N and δV waveforms for different axial carrier lifetime gradient characterised by parameter α ($\bar{\tau} = 2\ \mu s$ is assumed). (a) $\alpha = -160\ cm^{-1}$; (b) $\alpha = -80\ cm^{-1}$; (c) $\alpha = 0$; (d) $\alpha = 80\ cm^{-1}$; (e) $\alpha = 160\ cm^{-1}$.
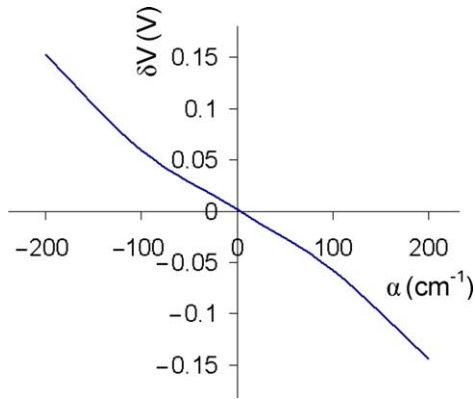
Fig. 5. A simulated dependence of δV on parameter α ($\bar{\tau} = 2\,\mu s$ is assumed) at $t = 40\,\mu s$ from opening the circuit.

In diode structures with the axial carrier lifetime gradient, an internal carrier concentration gradient is developed due to non-uniform recombination, which influences excess carrier distribution. The carrier flow from an area of higher carrier concentration decreases the rate of decrease of carrier concentration on the side with the lower carrier lifetime and increases the rate of carrier concentration decrease on side with the higher carrier lifetime. An additional voltage drop $\delta V(t)$ connected with non-uniform recombination develops relatively quickly and seriously influences the voltage decay waveform. It follows from the simulations that the absolute value of the voltage drop δV increases with increasing absolute value of carrier lifetime gradient as demonstrated in Fig. 5.

In the case of diode structures with axial carrier lifetime distribution, the voltage decay waveform can be divided into three parts, as indicated in Fig. 6. At the beginning of the process (part I), the carrier lifetime τ_I can be determined using (1). The value of τ_I is relatively close to (but higher than) what can be found from (8). During this phase of the process, the internal electric field increases, which results in an increase of the voltage drop δV given by (12). After sometime, a relatively constant excess carrier gradient is developed in the diode base

Fig. 7. Shape of the voltage decay waveforms during OCVD measurements on samples with a high axial carrier lifetime gradient in the base of the diode structure.

and the voltage drop δV is practically constant. In this phase of the transient process, the carrier lifetime τ_{II} can be determined using (1). The value of τ_{II} is connected with the mean value of carrier lifetime $\bar{\tau}$ (close to $\bar{\tau}/2$ under high injection conditions). At the end of the process (part III), there is a tile connected with relaxation of the internal electric field due to carrier lifetime gradient and it cannot be used for determining the low-injection carrier lifetime. If the carrier lifetime gradient is very high, the voltage decay waveform is a little changed and a local minimum may appear between part I and part II, as indicated in Fig. 7. Similar voltage decay waveforms are known from OCVD measurements on ion irradiated diode samples, where a very high carrier lifetime gradient was created [6].

The voltage decay waveforms measured on of this kind have also been found experimentally also on diodes diffused with iridium from the P^+-emitter side. The high injection carrier lifetime was measured using on-state current density 10 A/cm^2 (forward current rectangular pulses 200 μs in width with the edge shorter than 100 ns were applied with repetitive frequency 50 Hz). An example of the voltage decay waveform (measured using a digital oscilloscope with input impedance 10 MΩ) is
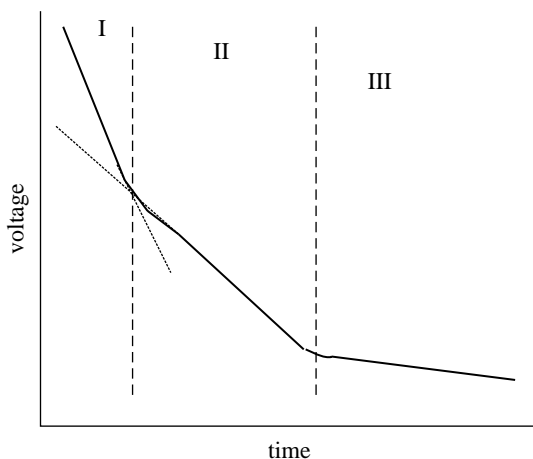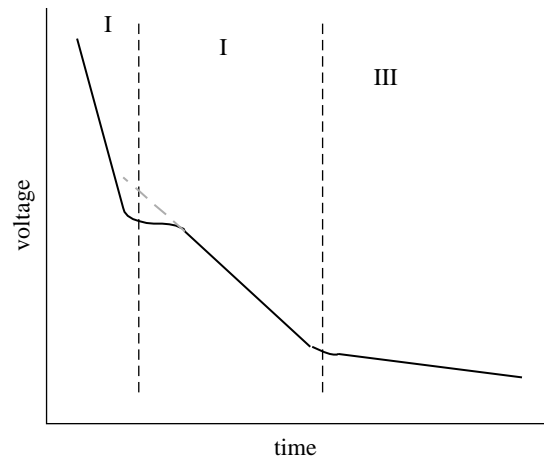

Fig. 6. General shape of voltage decay waveforms during OCVD measurements on samples with an axial carrier lifetime gradient in the base of the structure.
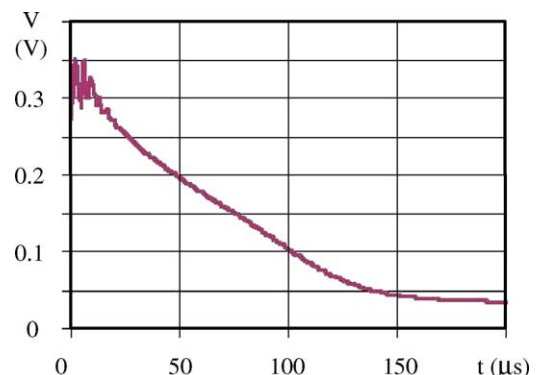

Fig. 8. An example of the voltage decay waveform measured on a diode sample diffused with iridium.

shown in Fig. 8. The waveform is in a relatively good agreement with the voltage decay type described in Fig. 6 for the case of an axial carrier lifetime gradient with carrier lifetime decreasing from the P^+ to the N^+ emitter.

5. Conclusions

From the analysis of the transient processes during OCVD measurements it follows, that for diode samples with an axial carrier lifetime gradient, the waveform of the voltage decay is strongly influenced by the excess carrier gradient induced due to inhomogeneous recombination. Under conditions of exponential distribution of carrier lifetime in the diode base, it is possible to obtain from the dV/dt slope in the middle part of the OCVD process an effective carrier lifetime relating to the mean value of the carrier lifetime (high injection) in the base of the diode. Lowever the voltage decay waveform is influenced by the carrier lifetime distribution. The tail of the OCVD voltage decay waveform depends mostly on the internal electric field due to the carrier lifetime gradient and cannot be used for determining the low injection carrier lifetime.

References

[1] S.R. Lederhandler, L.J. Giacoletto, Measurement of minority carrier lifetime and surface effects in junction devices, Proceedings of the IRE 43 (1955) 477–483.

[2] E. Di Ziti, G.M. Bisio, Determination of silicon power diode recombination parameters by combining open circuit voltage decay and storage time-reverse recovery data, Solid State Electronics 34 (1991) 771–780.

[3] Y.C. Gerstenmaier, A study on the variation of carrier lifetime with temperature in bipolar silicon devices and its influence on device operation, Proceedings of the ISPSD'94, 1994, p. 271.

[4] J. Vobecky, P. Hazdra, V. Zahlava, Open circuit voltage decay lifetime of ion irradiated devices, Microelectronics Journal 30 (1999) 513–520.

[5] M. Cernik, V. Benda, DIMOWIN—modelling diode reverse recovery process for education, Proceedings, of the ISPS'98, 1998, pp. 133–136.

[6] P. Hazdra, et al., Blocking capability of power P-i-N diodes irradiated by hydrogen and helium ions, Proceedings of the ISPS'2000, 2000, pp. 57–64.